

Inelastic Response Compatible Kanai-Tajimi Spectrum to Conventional Design Spectrum

Jun Kanda

John Hopkins University, Baltimore, MD USA

Ryoji Iwasaki

University of Tokyo, Tokyo, Japan

INTRODUCTION

It has been common to generate simulated earthquake ground motions with specified spectral characteristics both in seismic design procedures and in seismic safety evaluations. The Kanai-Tajimi(K.T.) spectrum has been widely used in parametric studies or safety evaluation because of its simplicity in the formula(Sues, R.H. et al 1985). Authors also have examined the inelastic responses based on the K.T. spectrum to reduce into a fairly simple form (Kanda et al 1989).

On the other hand target spectra have often been used in design procedures for important structures such as nuclear power plants. When a structure is designed against simulated motions fitted to the conventional design spectra and its safety is discussed by applying simulated motions specified by the K.T. spectrum, the difference in response characteristics between two input models have to be examined beforehand. In other words, there is a potential need to clarify the relationship between the K.T. spectrum model and the conventional design spectrum model not only in the elastic response but also in the inelastic response. This paper aims at proposing a reduction formula from a conventional design spectrum to a compatible K.T. spectrum focusing on the inelastic responses.

INELASTIC RESPONSES OF K.T. SPECTRUM MODEL

Response spectra for the average of three sets of ten simulated motions specified by K.T. spectrum and various envelope shapes corresponding to three earthquake magnitudes are shown in Fig.1 with typical parameter values η and f_G which are defined in the K.T. spectrum as follows,

$$S(f) = S_0 \frac{1 + \left(2\eta \frac{f}{f_G}\right)^2}{\left(\left(1 - \frac{f}{f_G}\right)^2\right)^2 + \left(2\eta \frac{f}{f_G}\right)^2} \quad (1)$$

Least squares fit lines with a corner frequency f_3 are also shown in dotted lines in the figure. Fitting was performed in the frequency range between 0.2Hz to 10Hz. In the frequency range lower than f_3 the velocity response becomes constant and the slope in the frequency range higher than f_3 changes with η . Difference due to the duration time or the envelope shape is not significant.

The corner frequency f_3 can be estimated from f_G in a linear form as shown

in Fig.2. Least squares fit line, obtained for the 27 plots with three cases for f_G , and the earthquake magnitude, may be expressed as

$$f_3 = 0.437 + 0.758 f_G \quad (2)$$

As may be expected from Fig.1 the K.T. spectrum can be converted to the design spectrum form easily but the conversion from the design response spectrum to the K.T. spectrum model has some limitations.

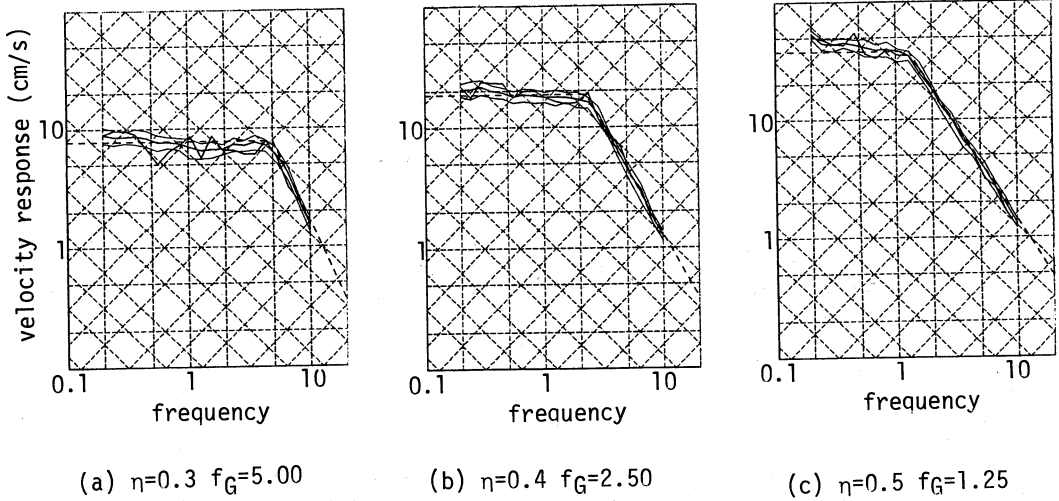


Fig.1 Response spectra for Kanai-Tajimi model with various parameters

When the inelastic responses are examined in terms of the equivalent elastic response Q which is defined as the hypothetical elastic response having the same potential energy as the inelastic response on the load Q -deflection diagram, Q vs. the peak acceleration, a , can be represented by the rectilinear approximation, i.e., straight lines passing the point (a_y, Q_y) , where a_y is the average peak acceleration causing the yield point response Q_y (Kanda et al 1987, Kanda et al 1989). Extensive studies have been carried out for six-degree-of-freedom lumped mass models with the normal bi-linear(N.B.) and the origin oriented hysteresis models for various fundamental frequencies and K.T. spectrum parameters as variables to reduce a simple formula(Kanda et al 1989). Similar numerical studies for the single-degree-of-freedom model lead to the same formula with different constants as follows,

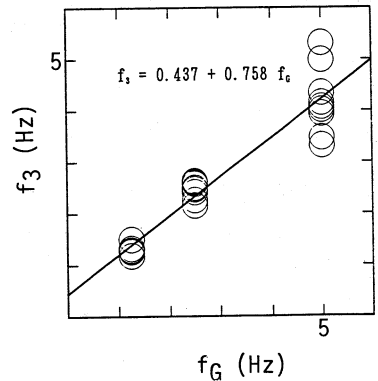


Fig.2 Relationship between the corner frequency f_3 and the predominant frequency f_G for the K.T. model

$$\left(\frac{Q^*/Q_y}{a/a_y} \right) \text{ at } Q^*=4Q_y = \left(A + \left(\frac{B}{f_G/f_o + E} \right) C \right)^D \quad (3)$$

A=0.0888, B=1.25, C=5.36, D=0.349, E=1.04 for N.B. and
 A= 1.20, B=1.92, C=5.27, D=0.361, E=1.08 for O.O.

where f is the fundamental frequency of structure.

Numerical results are shown in Fig.3 with eq.(2) and previous results for 6DOF models. Various techniques for the estimation of the response spectra based on the elastic response spectra have been reported. In order to compare the consistency of eq.(3), Miyama's formula (Miyama et al 1989) was applied, where the same hysteresis rules with the second stiffness after the yield point of $1/8$ of the initial as the computation described above were used. In Miyama's cases all elastic response spectra were expressed as the combination of three portions, i.e., the constant response displacement, the constant response velocity and the constant response

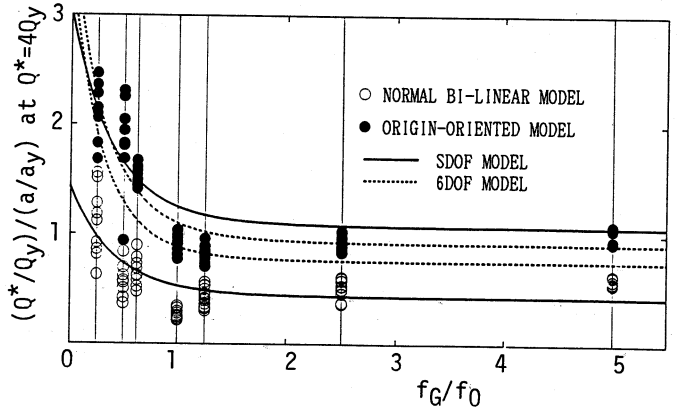


Fig.3 Relationship between the slope of equivalent elastic response against the peak acceleration and f_g/f_0

acceleration portions, for the simplification. As seen in Fig.2, the response spectra for the K.T. model do not have the constant response displacement and the slope in the higher frequency range ($f > f_3$) is somehow steeper than the constant response acceleration case depending mostly on the η value in eq.(1).

The comparison was made for two types of hysteresis rules with $f_G = 5.0, 2.5$ and 1.25Hz in Fig.4. The ductility factor was calculated for the frequency f_0 with the input yield ratio a/a_y as parameters by applying eq.(3).

Miyama's proposed formula can be summarized as,

For Normal Bi-linear

$$r = \mu^{-1.081} - (\mu^{-1.081} - \mu^{-1.361}) \left[u(f_2 - f) \exp(5 \log(\frac{f}{f_2})) + u(f - f_2) \exp(-10(\log(\frac{f}{f_2}))) \right] + u(f - f_3) \times 0.15 (\mu - 1)^{0.2} (\log \frac{f}{f_3})^{0.7} \quad (4)$$

For Origin Oriented

$$r = \mu^{-0.816} - (\mu^{-0.816} - \mu^{-1.068}) \left[u(f_2 - f) + u(f - f_2) u(f_2' - f) \frac{\log f_2' - \log f}{\log f_2' - \log f_2} \right] + u(f - f_3) (\mu^{-0.476} - \mu^{-0.816} + 0.065 \log f) \left[u(f - f_3') + u(f_3' - f) \frac{\log f - \log f_3}{\log f_3' - \log f_3} \right]$$

where $f_i' = (0.2\mu + 0.8)f_i$, $u(x) = \begin{cases} 0 & (x < 0) \\ 1 & (x \geq 0) \end{cases}$,

μ is the ductility factor, r is the de-amplification factor, i.e. the inverse of a/a_y . f_2 value is a corner frequency between the constant displacement portion and the constant velocity portion and f_3 is the corner frequency between the constant velocity portion and the constant acceleration portion. f_2 value was set to the lowest frequency 0.2Hz when the constant displacement portion is not in existence and f_3 value was obtained from eq.(2).

For the normal bi-linear model, eq.(4) gives larger estimation of ductility factor throughout for most cases than the estimation based on eq.(3). For the origin oriented model, eq.(4) gives smaller estimation especially in the lower frequency range with high a/a_y ratio.

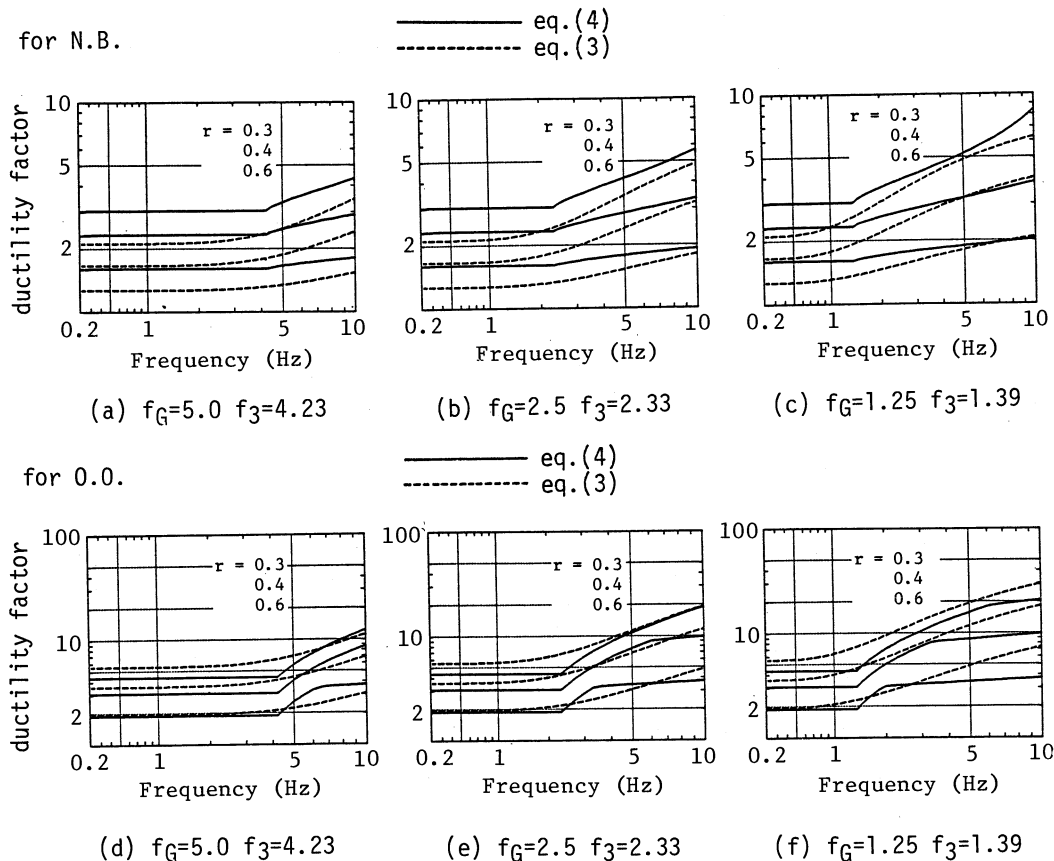


Fig.4 Ductility factor estimations due to eq.(3) and (4)

DESIGN SPECTRUM COMPATIBLE K.T. MODEL

Because of the response spectral nature of K.T. model, it is obvious that the constant response displacement portion can not be represented by the K.T. model. However for certain frequency ranges the K.T. model may represent not only the elastic but also the inelastic response in a compatible manner to the simulated motions fitted to the conventional design spectra.

Typical three cases of the Ohsaki spectrum were examined, i.e. (a) $M=6.5$, $\Delta =7.2$ km, (b) $M=7.0$, $\Delta =20$ km, (c) $M=8.4$, $\Delta =90$ km as shown in Fig.5, where Δ is the

epicentral distance. The corner frequency, the right end frequency of constant velocity portion, f_3 for each case is 5.75Hz, 3.68Hz and 2.87Hz respectively.

Inelastic responses were examined in the similar manner to the previous chapter. Computation results in terms of the ductility factor with a_y/a as a parameter as the average of ten simulated motions for the design spectrum of Fig.5 are shown in Fig.6, together with the estimation based on eq.(3) where f_g is obtained from eq.(2) by substituting f_3 value and the estimation due to Miyama's formula.

Miyama's formula eq.(4) gives a good representation especially for the N.B, but the general tendency of the simulated results may be considered to be explained also by eq.(3) based on the K.T. model.

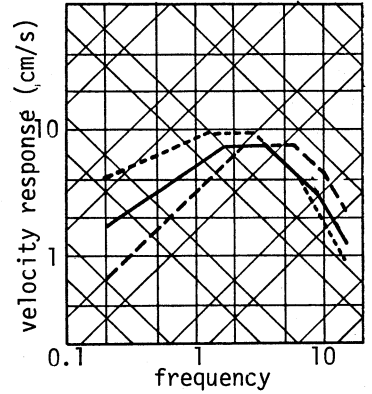
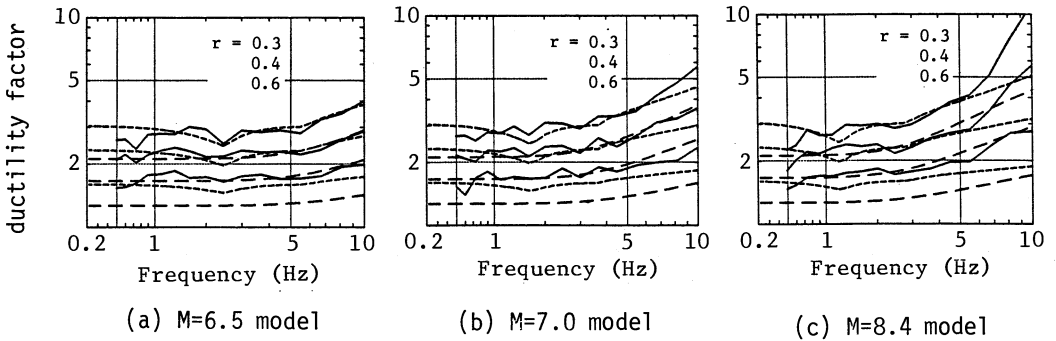


Fig.5 Three cases of Ohsaki Spectra

--- for M=6.5
 — for M=7.0
 ··· for M=8.4

for N.B. — simulation
 ··· eq.(4)
 --- eq.(3)



for 0.0. — simulation
 ··· eq.(4)
 --- eq.(3)

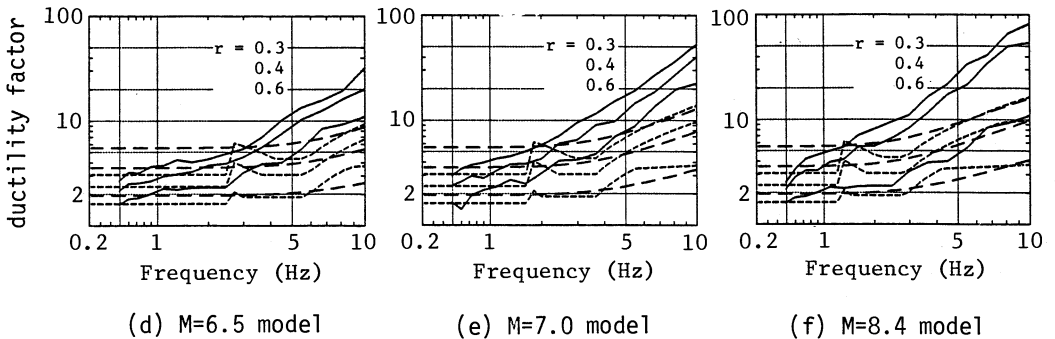


Fig.6 Ductility factor spectra for Ohsaki spectral models with $a_y/a=0.3, 0.4$ and 0.6 in comparison with estimations due to eq.(3) in dashed lines and eq.(4) in dotted lines

CONSIDERATIONS AND CONCLUSIONS

The design spectrum does not necessarily represent the spectral characteristics of the actual earthquake ground motions and some modification could be incorporated by the engineering judgment. Significant discrepancies between the conventional design spectrum and the K.T. model clearly appeared in the low frequency range. Although the inelastic response characteristics at a high frequency such as the fundamental natural frequency of the nuclear power plant buildings may only be influenced insignificantly, further discussions and careful examinations on low frequency spectral characteristics of the actual earthquake ground motions are important for the rationalization of the design procedure and also for the seismic safety assessment.

The difference of inelastic responses due to the hysteretic rules was significant as seen in Figs.3,4 and 6. This difference was much less for the multi-degree-of-freedom model (Kanda et al 1989) and the extremely large ductility factor in the high frequency range may not directly applicable to the multi-story buildings.

The K.T. model could be substituted to a set of simulated motions fitted to the design spectra with the aid of the relationship between the dominant frequency in the K.T. model and the corner frequency in design spectra expressed by the eq.(2).

The limitation for the compatibility exists especially in the lower frequency range but the difference in the shape of elastic response spectrum does not influence considerably on the inelastic response in the frequency range between 0.5Hz and 5Hz.

Following conclusions could be drawn from this numerical study.

- (a) Based on the examination of response spectra of the Kanai-Tajimi model earthquake ground motions, the relationship between the dominant frequency in the K.T. model and the corner frequency in the rectilinear response spectral approximation can be reduced into a linear form.
- (b) This relationship can be adopted to make a design spectrum compatible K.T. model.
- (c) General tendencies of inelastic response spectra may be represented by the K.T. model with a reduced formula for the rectilinear relationship between the equivalent elastic response and the input intensity.

ACKNOWLEDGEMENT

Authors are indebted to Mr. H. Kobayashi for his help in computation and preparing figures.

REFERENCES

- Hisada,T., Ohsaki,Y., Watabe,M. and Ohta,T. (1978). Design Spectra for Stiff Structures on Rock. Proc. 2nd Int. Conf. on Microzonation, Vol.III, San Francisco, pp. 1187-1198
- Kanai,K. (1961). An Empirical Formula for the Spectrum of Strong Earthquake Motions. Bull. Earthq. Inst., Univ. of Tokyo, Vol.39, pp. 85-95
- Kanda,J., Iwasaki,R. and Sunohara,H. (1987). Stochastic Evaluation of Inelastic Seismic Response of a Simplified Reactor Building Model. Trans. 9th Int. Conf. Str. Mech. in Reactor Tech., K7, pp. 403-408
- Kanda,J. and Iwasaki,R. (1989). Stochastic Evaluation of Inelastic Seismic Response for Multi-Degree-of-Freedom Lumped Mass Models. Proc. 9th World Conf. on Earthquake Engineering, Vol. VIII, pp. 797-804
- Miyama,T., Kanda,J. and Iwasaki,R. (1989). Inelastic Response Spectra for Typical Hysteretic Systems Calculated from Elastic Response Spectra. Proc. 9th World Conf. on Earthq. Engineering, Vol. V, pp. 153-158
- Sues, R.H., Wen, Y.K. and Ang, A.H.S. (1985). Stochastic Evaluation of Seismic Structural Performance. J. Str. Eng. Proc. ASCE, Vol.III, pp. 1204-1218